JOURNAL OF MATERIALS SCIENCE 24 (1989) 2099–2109

The effects of contact conditions on impact tests on plastics

N. J. MILLS
Department of Metallurgy and Materials, University of Birmingham, PO Box 363, Birmingham B15 2TT, UK

P. S. ZHANG
The Research Institute for Strength of Metals, Xi'an Jiatong University, Xi'an, China

The causes of the force oscillations observed in instrumented impact tests were investigated. Vibrational modes are excited in cantilever-beam specimens by the initial contact between the striker and the specimen. Although a one-dimensional mass and spring model can predict the oscillations qualitatively, the predicted forces are too large by a factor of two for slender cantilever beams, but approximately correct for lower aspect ratio beams. Computer models can predict the whole of the force deflection curve, but no one-dimensional model can realistically model all the details of the vibrations of a beam specimen. One effective way of reducing the oscillations was to introduce a high hysteresis rubber between the striker and specimen. This was found to produce more meaningful force-deflection or stress–strain curves for polystyrene, without changing the values of the failure stress.

1. Introduction

Instrumented impact tests on plastics have become popular recently both because of the availability of commercial equipment [1, 2] and because of the need to obtain fracture information under impact conditions. The results of tests on notched bars can be analysed to give fracture mechanics information [3, 4] or those on unnotched bars or discs can give stress–strain curves at high strain rates [5].

Most authors observe force oscillations on top of the expected signal. These oscillations are more marked when brittle glassy polymers in thicknesses exceed 3 mm are tested [5–7]. We were concerned to investigate fully the source of the oscillations and to see whether they can be predicted. This is relevent to the understanding of impact failures in larger plastics structures, where short-lived force peaks may trigger failure processes such as crazing.

We had previously studied and analysed the force oscillations that occur when plastic protective helmets are involved in high speed impacts [8]. It has been found that both the contact stiffness between the striker and the plastic product, and the product mass determined the size of initial force peaks, and mathematical modelling had been used successfully to predict the force variations [9]. Therefore we look for similar effects in impacts on plastic cantilever beams (an unnotched Izod impact test). Polystyrene was chosen for study because of its brittle nature, and the possibility that crazes could be initiated by force transients. We could then investigate whether the size of initial force transients affected the impact strength.

2. Equipment design and experimental details

2.1. Selection of the unnotched Izod test

The reason for carrying out an impact test on a cantilever beam of rectangular cross section were that this is one of the simplest experimental geometries, and the theory for the vibration of a cantilever beam is well established [10, 11]. If the specimen is not notched or cracked then none of the complexities of stress concentration factors or fracture mechanics apply. This is important if we are trying to establish as quantitative theory for the magnitude of force oscillations in impact.

One reason for selecting an Izod rather than a Charpy 3-point bend test was that a greater range of specimens lengths could be used. Specimens of dimensions 120 mm × 20 mm × 4 mm were prepared by injection moulding on a Battenfeld machine, with cavity pressure control to ensure reproducibility of the moulding conditions. With a clamped length of 20 mm, it was possible to have cantilever lengths of 40, 60, 80 and 100 mm, whereas the impact point was always 30 mm from the clamped end.

2.2. Design of the pendulum and force measurement system

The equipment was based on an Avery Izod impact tester of 10 ftlb capacity. The original 200 mm long pendulum has two large brass masses attached to either end of a rod-like striker. When an accelerometer was attached to the rear face of one of the brass masses it was soon found that sound waves travelling

0022–2461/89 $03.00 + .12

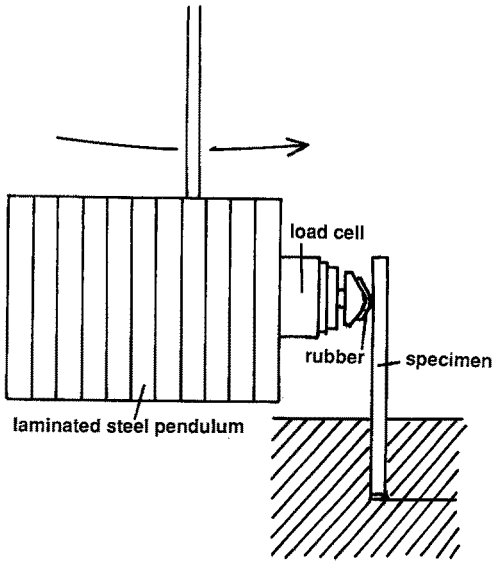

Figure 1 The laminated steel pendulum, quartz load cell and striker used in Izod tests.

in the brass swamped the signal from the impact. Therefore a completely new pendulum and force measurement system was constructed (Fig. 1).

1. The pendulum mass is a rectangular block of laminated steel. Eleven 7 mm thick steel plates are bonded together with a toughened acrylic adhesive (Permabond F241), which is a low modulus material. Therefore any sound waves in the steel are either absorbed at the steel–adhesive interfaces, or if they are reflected back the reflection occurs in $\sim 3\,\mu$sec, which is a shorter time scale than any other event. In practise sound waves in the 1.14 kg pendulum were not a problem.

2. A Kistler model 9321 quartz piezoelectric force cell was used to measure the force. The mass of the steel striker bolted to the front of the force cell is 16 g. The cell has the extremely high stiffness of $9 \times 10^8\,\mathrm{Nm}^{-1}$ and an initial resonant frequency of 57 kHz. The additional 16 g reduces the resonant frequency to 31 kHz or a period of 32 μsec.

3. The output of the force cell is taken through a Kistler charge amplifier with a cut-off frequency of 180 kHz. Consequently this does not modify the load cell output. Some authors [12] have used filters at 2 kHz to smooth the output from impact tests; however they are filtering out real signals. The signal then passes to a Datalab model 902 transient recorder which is set to sample at intervals of 10 μsec and has an 8 bit Analog to Digital converter. The data was analysed with an IBM or Amstrad microcomputer.

4. The contact with the sample is either a steel cylindrical surface of radius approx 3 mm and length 15 mm, or the same covered with either 1.5 mm of polyurethane rubber of hardness IRHD = 78, or 3.5 mm of polyurethane rubber of hardness IRHD = 52. These correspond to shear moduli of approximately 2.5 and $0.5\,\mathrm{MN\,m}^{-2}$.

The measuring system was calibrated before use. A static compressive load of 98 N was applied to the load cell, and the computed force found to agree with this to within 1%. When a pendulum of mass m falls through a height h from rest, the conservation of energy gives

$$mgh = \tfrac{1}{2}mv^2 + \tfrac{1}{2}I\omega^2 \qquad (1)$$

where v is the velocity of the mass and ω the angular velocity. If the mass is concentrated at the end of the pendulum of length L, then the moment of inertia $I = mL^2$, and the linear and rotational kinetic energy terms are equal. Hence the velocity is given by

$$gh = v^2 \qquad (2)$$

where g is the acceleration of gravity.

The acceleration of the striker is calculated from the impact force F using Newton's 2nd Law. Numerical integration can then be used to calculate in turn the velocity and position of the striker. Further checks of the accuracy of the integration procedure were made during the dynamic contact stiffness measurements described in section 2.4. During the Izod tests the pendulum has a considerably greater kinetic energy than that needed to break the specimen, so the percentage velocity change of the striker is not that high.

2.3. Larger scale cantilever impact tests

In a simple spring and mass model of dynamic effects in impact tests [13] the shape of the force time response depends on the ratio of the contact stiffness between the specimen and striker, and the bending stiffness of the specimen. If this ratio can be made very large then an isolated "bounce" will occur and the size and time duration of this can be measured accurately. Therefore we carried out tests on solid cylinders of polypropylene and PVC that were 32 mm in diameter and had a cantilever length of 600 mm. The 1.81 kg striker was half of aluminium cylinder of 50 mm radius, with its axis at 90° to that of the cantilever (Fig. 2). The ratio of the two stiffnesses turned out to be the order of 1000, which is sufficient for the impact to be a series of bounces. The striker could fall vertically between wire guides, and therefore achieve a

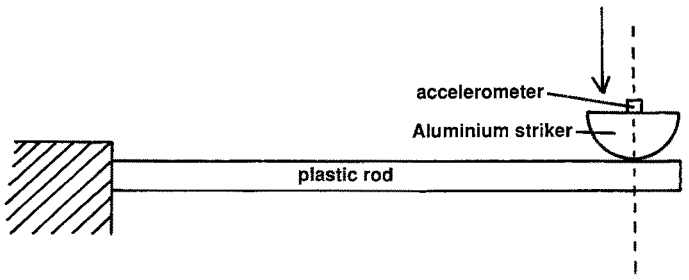

Figure 2 The freely falling hemi-cylindrical aluminium striker and quartz accelerometer used in impacts on large cantilever beams.

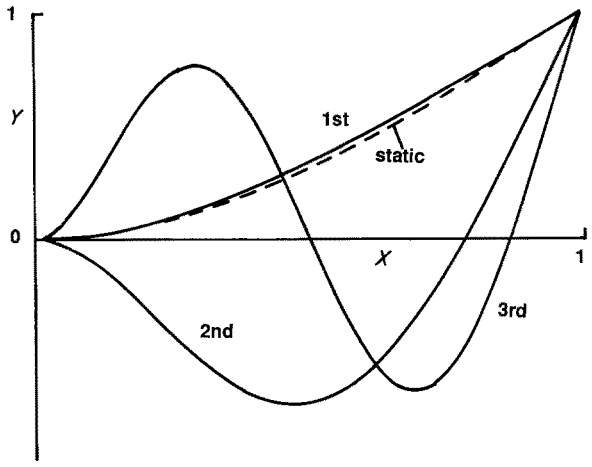

Figure 3 The first three modes of vibration of an elastic cantilever beam compared with the deflection of a beam loaded statically at the free end. The deflection of the free end is normalized as 1 unit.

range of velocities before impact (this was an adaptation of some helmet testing equipment). A Kistler "Piezotron" accelerometer attached to the top of the cylinder was used to monitor the acceleration, and the signal passed to a transient recorder and IBM microcomputer as in the other tests.

2.4. Contact stiffness and coefficient of restitution measurements

Initially contact stiffness measurements were made on a time scale of 1 min using an Instron compression testing machine, and loading the rubber or polystyrene between a flat steel table and the striker nose. In the case of the large cylindrical beams these were symmetrically loaded between two cylindrical strikers. However the viscoelastic nature of these polymers means that the contact stiffnesses will be considerably higher on the 1 to 5 msec time scale of an impact test. Therefore a steel beam of cross section 40 × 20 mm was clamped in the Izod machine and the pendulum allowed to impact this from a low drop height.

As a further check, the coefficient of restitution of the materials was measured by dropping a 3 g steel sphere from 0.25 m onto the materials which were fixed with cyanoacrylate adhesive on a solid steel base, and measuring the rebound height. The coefficient of restitution is the ratio of the rebound to the drop height.

3. Theory

3.1. Vibrations of a cantilever beam

When a cantilever beam of length L is loaded statically at its free end by a force F the bending moment M varies according to

$$M = FL(1 - x/L) \tag{3}$$

where the position variable x is zero at the clamped end (Fig. 3). The differential equation for the deflection y of the beam

$$\frac{d^2y}{dx^2} = \frac{E}{MI} \tag{4}$$

where E is Young's modulus and I the second moment of area, can be integrated to give the deflection as

$$Y = \tfrac{1}{2}(3X^2 - X^3) \tag{5}$$

where X is the normalized position equal to x/L and Y the normalized deflection equal to y/y_L where y_L is the end deflection. Consequently the average deflection of the beam $\bar{Y} = 3/8$.

When the same cantilever beam is loaded dynamically the partial differential equation for flexural waves on it is

$$\varrho A \frac{\partial^2 y}{\partial t^2} + EI \frac{\partial^2 y}{\partial x^4} = 0 \tag{6}$$

where ϱ is the density of the material and A the cross-sectional area of the beam. One solution of Equation 6 is a resonant vibration with angular frequency ω, where ω is given by

$$\omega^2 = \frac{EI}{\varrho A} m^4 \tag{7}$$

The boundary conditions of zero shear force and bending moment at the free end of the cantilever lead to the condition that

$$\cosh mL \cos mL + 1 = 0 \tag{8}$$

The solutions to Equation 8 are $mL = 1.8751$ and 4.6941 for the 1st and 2nd modes of vibration, respectively. Equation 7 and 8 determine the resonant frequency. The deflection y of the beam is given by

$$y = C \cos \omega t \times [\cosh mx - \cos mx + B(\sinh mx - \sin mx)] \tag{9}$$

where $B = -(\cosh mL + \cos mL)/(\sinh mL + \sin mL)$ and C is a constant.

Different modes of vibration can be excited, depending on where the beam is struck. If we assume that when the beam is struck at the free end only the first vibration mode is excited, then the normalized mean deflection of the beam $\bar{Y} = 0.392$; this is only 4.5% larger than the static case. The result will change however if a combination of vibration modes is excited.

Williams [14] defines the equivalent mass of an impacted beam, as the concentrated mass at the end of the beam has the same kinetic energy as the beam. He also assumes that most polymer beams have the same coefficient of restitution of 0.5. Now the collision between a striker and a polymer beam is an anelastic process, and the coefficient of restitution can vary. The total kinetic energy of the two bodies is not conserved but the momentum is conserved. It seems more logical to define an effective mass that has the same momentum as the beam. Therefore the beam of mass M_2 and known momentum will be replaced by a concentrated mass M_2' at the end of the beam that has the same velocity as the end of the beam, and the same momentum. Using this definition the effective mass of a cantilever beam in the first vibration mode is

$$M_2' = 0.392 M_2 \tag{10}$$

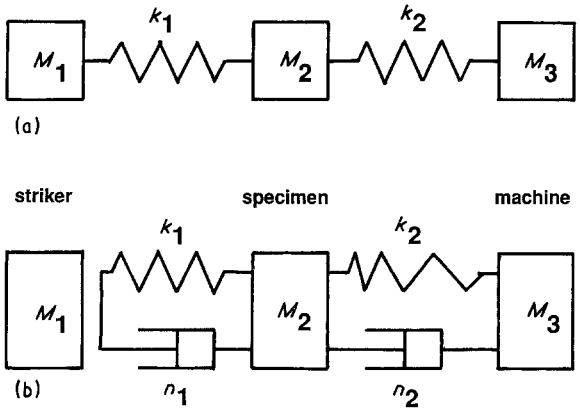

Figure 4 (a) Williams' one-dimensional mass and spring model. (b) Our one-dimensional mass, non-linear spring and damper model. The striker mass M_1 can separate from the spring k_1.

3.2. Analysis of a one-dimensional mass/spring model

Figure 4a shows Williams's model [13] of the impact process. It consists of a striker of infinite mass M_1 travelling initially at velocity v, an effective specimen mass M_2' and a machine mass M_3 which is also infinite. The linear springs k_1 and k_2 represent the contact stiffness between the striker and specimen, and the bending stiffness of the specimen, respectively. The solution for the contact force F, is

$$\left(\frac{1 + k_1/k_2}{k_1/k_2}\right)\frac{\omega F}{k_2 v} = \frac{k_1}{k_2}\sin \omega t \qquad (11)$$

where the angular frequency $\omega^2 = (k_1 + k_2)/M_2'$. In the limit as $k_1 \gg k_2$ and for short times where the ωt team can be neglected, Equation 11 simplifies to

$$F = v(M_2' k_1)^{1/2} \sin \omega t \qquad (12)$$

Consequently there is an initial force peak of magnitude F_m, where

$$F_m = v(M_2' k_1)^{1/2} \qquad (13)$$

The solution fails once the initial "bounce" is over, because in reality the specimen loses contact with the striker, but in the model the spring remains attached and the force F becomes negative.

The model is one-dimensional; it assumes that the cantilever deflection is always of the same shape, so that an effective cantilever mass can be defined. If flexural stress-waves propagate down the beam, or if a range of modes of vibration are excited then the model will be inaccurate.

3.3. Computer solutions of a one-dimensional mass/spring damper model

Once features such as a finite mass striker or the possibility of loss-of-contact between the striker and the specimen are introduced, then the model equations become too complex to solve analytically. However it is relatively easy to solve the equations by computer, using successive applications of Newton's law at intervals of 1 μsec [9]. To obtain as realistic as possible a model, the following features were included (Fig. 4b).

1. The striker loses contact with the specimen if the force F_1 falls to zero.
2. There is a non-linear spring for the contact between the striker and the specimen. Above a force limit $F_{Lim} \sim 100$ N the spring is linear but below this the force–distance relation is parabolic. There is no change of slope at the transition point. The justification is the measured contact behaviour (section 4.1).
3. There are dampers in parallel with both the springs. The justification is that there is hysteresis in the striker–specimen impact, and the vibrations in the cantilever are damped. Subsidiary measurements of the coefficient of restitution are used to evaluate the constants n_1. In the region where the spring k_1 is non-linear the constant n_1 is reduced proportionally to avoid a change in the ratio n_1/k_1, which represents a retardation time of the model.

No attempt was made to use multiple spring and damper models of the type used for the viscoelastic properties of plastics [15]; this is because the impact occurs on a particular timescale so single retardation time model should be adequate. One drawback is that the spring and damper values that model a material are a function of the impact speed; however this is a minor drawback given the simplicity of the model.

4. Results

4.1. Contact stiffnesses and bending stiffness

Figure 5 shows the force against compressive deflection graphs of the two polyurethane rubbers, for a dynamic test lasting 5 msec. There is a high degree of hysteresis, and the area under the curve on unloading (energy output) is far smaller than the energy under the loading part of the curve (energy input). The ratio of these energies is given in Table I, together with the slope of the linear part of the loading curve, which starts above 150 N. The energy ratios for the impacts agree well with the coefficients of restitution for the two rubbers. The energy ratio for the polystyrene is subject to error because both the drop height (8 mm) and the maximum deflection (68 m) are very small. The static loading stiffnesses are considerably smaller than the dynamic ones; this is expected for a viscoelastic polymer with high hysteresis.

The bending stiffness of the polystyrene Izod beams was calculated from the inital slope of the experimental force against deflection graphs (Section 4.4). The value obtained was 45 kN m^{-1}. Therefore in

TABLE I Dynamic contact data, Izod tests

Material	Dynamic loading stiffness (kN m^{-1})	Energy out/ energy in	Coefficient of restitution	Static loading stiffness (kN m^{-1})
3.5 mm soft polyurethane	360	0.02	0.02	250
1.5 mm hard polyurethane	1 430	0.24	0.20	750
4 mm polystyrene	14 800	0.16	0.90	2800

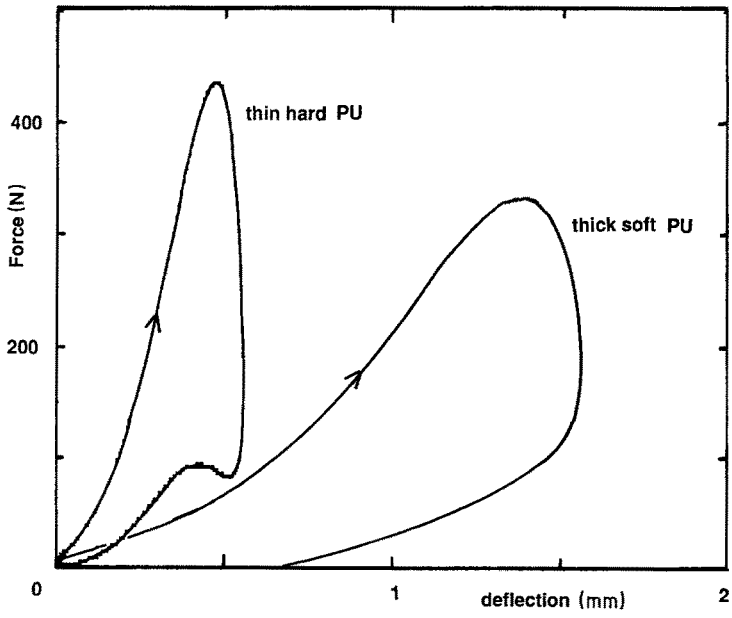

Figure 5 Experimental dynamic force deflection curves for the two polyurethane rubber layers used on the Izod striker.

comparison with the first column of Table I the contact stiffness is between 8 and 330 times the bending stiffness.

For the large cylindrical cantilever beams the contact stiffnesses and other data are given in Table II.

As the ratio of the (static) contact to bending stiffness is about 7000 for both polymers, this is much higher than in any of the Izod tests. The coefficient of restitution for a 3 g sphere impacting the flat plastic from 0.25 m is nearly double the energy ratio for the 1.8 kg cylindrical striker impacting the cylindrical cantilever beam from 0.2 m. In the latter case the force rises to 6 kN; the reasons for the low energy ratio are both that there is greater anelastic behaviour at higher stress levels, and that there may be losses in the lower anvil support.

The increase in contact stiffness from static to dynamic testing is greater (66%) for polypropylene than for PVC (31%) reflecting the greater damping factor in the semi-crystalline polypropylene. The tan δ damping factor was measured from the decay of the natural vibration of the beams as 0.07 for polypropylene and 0.02 for PVC.

4.2. Impacts on large cantilever beams

The purpose of testing large cantilever beams was to obtain conditions where an isolated initial force peak occurred. Figure 6 shows that this was indeed the case. For the PVC beam there is an initial peak followed by a second peak 3 msec later when contact between the beam and the striker recurs. For the polypropylene beam the initial peak has a more complex shape with a secondary shoulder on it, and there is no obvious secondary peak. The low level oscillations are artefacts, due to vibrations or sound wave reflections in the aluminium striker affecting the accelerometer on the upper surface of the striker.

When the impact velocity of the freely falling striker was varied over the range 1–4 $msec^{-1}$ the magnitude F_{max} of the initial force peak was found to vary linearly with the velocity (Fig. 7). This is expected from the Williams model, and indicates that the plastics are unlikely to have yielded at the contact region. Equation 13 can be used to predict the size of the maximum force, using the measured dynamic contact stiffness, and an effective mass given by Equation 10, for an impact velocity of 4 $msec^{-1}$. Table III shows that these predictions exceed the experimental values by a factor between 2.2 and 2.4. To see whether this is due to Williams' model ignoring the damping in the contact zone, a further calculation was made using the computer model (see section 4.4). In order to reproduce the experimental coefficients of restitution, the damper constants must be 50 Nsec m^{-1} for polypropylene and 27 Nsec m^{-1} for PVC. The revised predictions using this model, are respectively 5 and 7% less than the simpler William's model predictions. Thus the discrepancy is not due to ignoring damping, and

TABLE II Impact properties of large plastic cantilever beams

Property	Polypropylene	PVC	Comment
Diameter (mm)	31.0	32.7	
Mass of cantilever (g)	398	649	
Static bending stiffness (kN m^{-1})	1.0	2.5	
Static contact stiffness (kN m^{-1})	7700	14 500	
Dynamic contact stiffness (kN m^{-1})	12 800	19 000	
Energy out/energy in	0.29	0.41	
Coefficient of restitution	0.60	0.75	
F_{max} for $V = 4\,m\,sec^{-1}$ (kN)	2.4	4.0	
Predicted F_{max} (kN)	5.7	8.8	Equation 13
Predicted F_{max} (kN)	5.4	8.2	Computer model

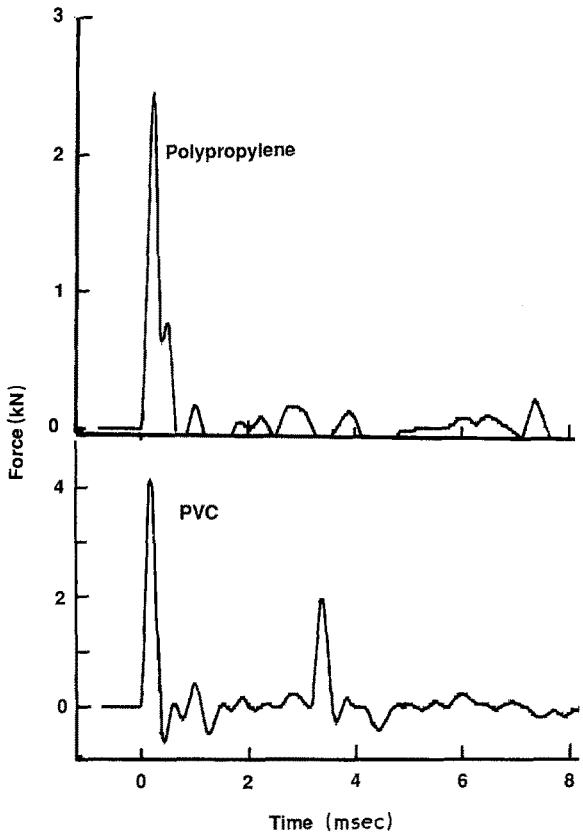

Figure 6 Striker force against time for impacts on the large PVC and polypropylene beams.

the theoretical predictions are a factor of two too large.

4.3. Impacts on small Izod specimens

If a steel striker hits a 40 mm long polystyrene beam directly then the force against time trace shows a great deal of oscillation (Fig. 8). Initially, there are high harmonics on a sine wave signal, but these decay more rapidly than the fundamental, so just prior to fracture only the fundamental vibration remains. This behaviour contrasts with the force against distance trace obtained when there is a 3.5 mm layer of the soft polyurethene rubber on the striker nose (Fig. 9). There are no oscillations visible until after fracture, when a high frequency oscillation occurs in the pendulum. If a thin rubber layer of the harder polyurethane rubber is used then about five damped cycles of the fundamental frequency of oscillation are visible on the trace (Fig. 9).

If the polystyrene cantilever is longer, then the oscillations become more marked, in spite of the presence of the thin polyurethane damper on the striker nose. Figure 10 shows a typical force against time trace for a 80 mm long cantilever. The impact point remains 30 mm from the clamp, but relative to the beam length the impact point is less far along the beam. The observed periods of oscillation T are plotted against the cantilever lengths L on logarithmic scales in Fig. 11. The data fit a relationship $T \propto L^3$. The vibrating-reed theory predicts that the period of the first mode of oscillation is given for a rectangular cross section beam of depth d and length L by

$$T = 6.19 \frac{L^2}{d}\left(\frac{\varrho}{E}\right)^{1/2} \quad (14)$$

This relationship is shown in Fig. 11 for a density $\varrho = 1200\,\mathrm{kg\,m^{-3}}$ and a Young's modulus $E = 4.0\,\mathrm{GN\,m^{-2}}$. The experimental data approaches the theoretical line as the beam length increases, but at a 40 mm length the times differ by a factor of 3.7. When the contact stiffness is far higher than the specimen bending stiffness, the Williams' theory predicts an angular frequency $\omega = (k_1/M_2')^{1/2}$. The effective mass M_2' in this model is 3/8 of the cantilever mass, which in turn is proportional to the cantilever length L. Consequently the periodic time is predicted to vary as $L^{1/2}$ Fig. 11 shows the predictions of the Williams' model for the thin rubber contact stiffness of $750\,\mathrm{kN\,m^{-1}}$. The experimental data approaches this line for the shortest beams. Overall it would appear that for 4 mm thick polystyrene beams the Williams' model could be valid for beams shorter than 30 mm, and the vibrating-reed theory is accurate for beams longer than 100 mm. In terms of the length to depth ratio of the beams, if this ratio is less than 8 Williams' theory applies, and if it exceeds 25 the vibrating-reed theory applies.

The force against time traces for 40 mm long cantilevers were processed to generate striker force versus

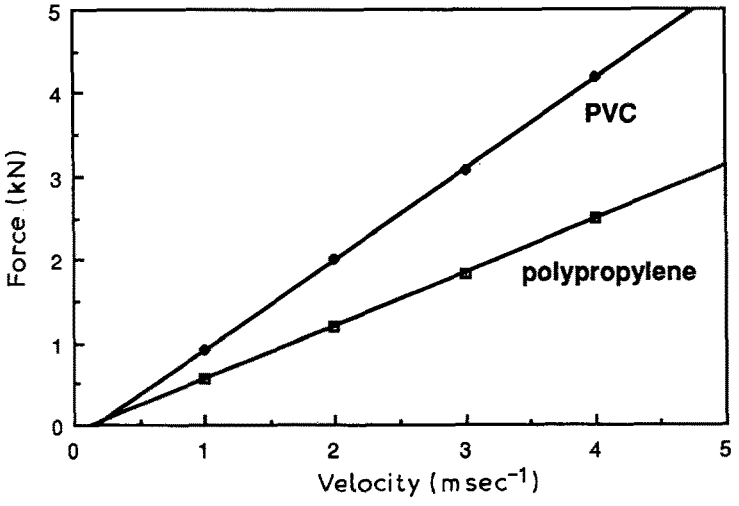

Figure 7 Variation of the initial force peak height F_m for impacts on large beams at different impact velocities.

TABLE III Fracture of polystyrene Izod bars

Contact condition	No. of samples	Failure force (N)	Failure deflection (mm)	Energy (J)	Failure time (msec)
Steel	7	182 ± 27	4.5 ± 0.8	0.45 ± 0.16	4.6 ± 1.2
Hard PU	6	158 ± 17	5.4 ± 1.0	0.47 ± 0.15	5.5 ± 1.3
Soft PU	6	165 ± 30	5.4 ± 1.0	0.48 ± 0.18	6.0 ± 1.1

The sample standard deviation of each measurement is given.

beam deflection graphs. Figure 9 shows these for the two rubber coated striker contact conditions. There is a clearly defined fracture point when the force falls to zero. The statistics of the tests are set out in Table III, where the force, deflection, energy input, and time at fracture are given.

The differences between the force and energy values are not significant; it is expected that the deflection at failure would increase by F_{max}/k_1 or 0.7 mm when the soft polyurethane rubber is used, and this will also cause the failure time to increase slightly.

As the force deflection graphs are reasonably linear, it is possible to calculate the failure strains in the bars using elastic stress analysis. This should be done with some caution because crazes have extended across 2/3 of the specimen width before fracture, and crazing is a form of localized yielding. The elastic theory of a cantilever relates the maximum strain e_m to the deflection x by

$$e_m = \frac{1.5dx}{L^2} \quad (15)$$

and the maximum stress σ_m to the force F by

$$\sigma_m = \frac{6FL}{wd^2} \quad (16)$$

where w is the width and d is the depth of the beam. As the specimens are identical in size, it is possible to relabel the curves in Fig. 9 as σ_m against e_m.

When this is done it is seen that the maximum stress (on the tensile surface at the clamp) is 100 ± 15 MN m^{-2}. This is double the value calculated for a bend test lasting 1 min in an Instron machine. The non-linearity of the curves in Fig. 11 before fracture is evidence of yielding so this value is an overestimate of the yield stress on a 5 msec time scale. Nevertheless the high stress, and the maximum strain 3.1 ± 0.6% shows that polystyrene is much stronger on a short timescale than it is in conventional tensile tests.

4.4. Computer modelling of impacts on a cantilever beam

The three mass plus two damped spring model of Fig. 4b was used to model the impacts. If the spring and damper constants are taken to be disposable then it is relatively easy to fit an experimental graph of the contact force against time. However if each of the constants is estimated from separate experiments then it is possible to check if the model is quantitatively correct.

The contact stiffnesses k_1 of the steel and rubber covered steel strikers were estimated from instrumented rebound tests (Fig. 5). Because of the high hysteresis of the rubbers, the dynamic loading stiffnesses (Table I) will be a combination of the elastic stiffness plus a large contribution from the damping. Therefore the "static" loading stiffness were used as a better estimate of the underlying elastic contact behaviour.

The contact damper constants n_1 were estimated from measurements of coefficient of restitution (Table I). These measurements used an impact velocity of 2.21 m sec^{-1}, whereas in the Izod tests the pendulum velocity at impact was 1.15 m sec^{-1}. A simplified version of the

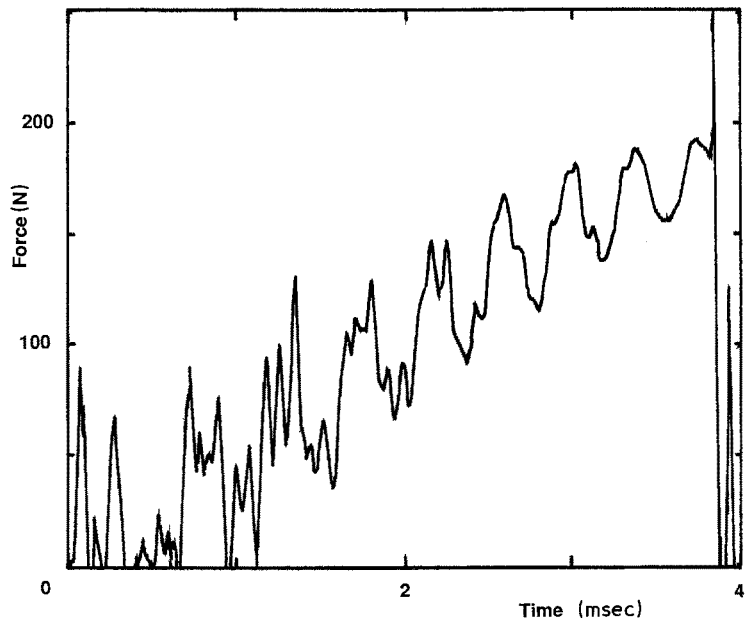

Figure 8 Striker force against time for the steel Izod striker on a polystyrene specimen of length 40 mn.

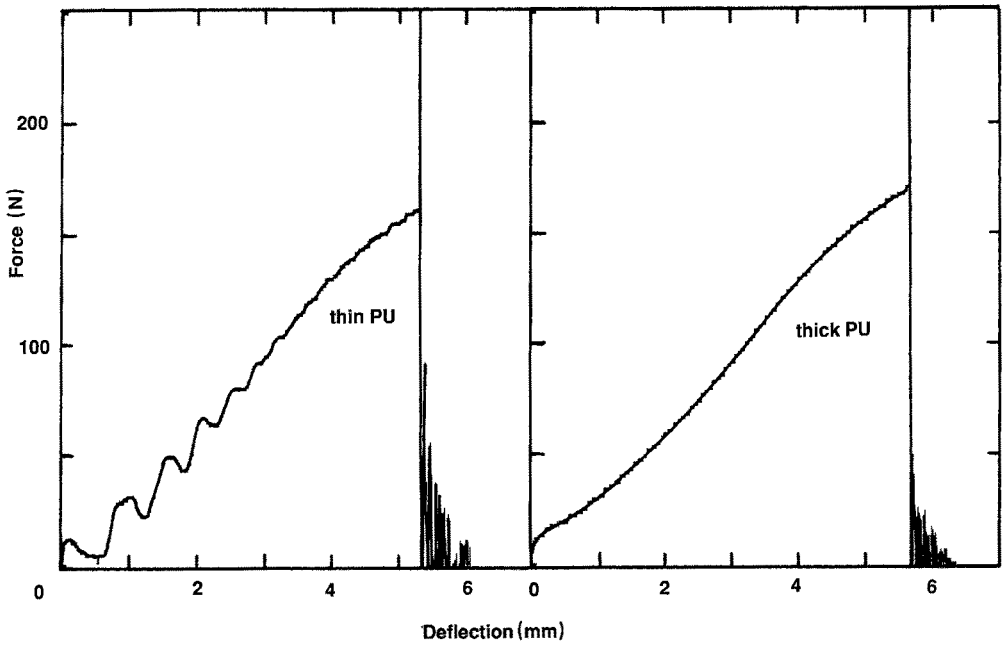

Figure 9 Striker force against striker movement for polyurethane covered Izod strikers hitting polystyrene beams of 40 mm length.

computer model (Fig. 4b) was used to find the n_1 value that gives the correct coefficient of restitution; the sphere mass M_1 was 5 g whereas the "specimen" mass M_2 was made infinite so that it represents the immovable support for the rebound test. Using the static k_1 values, and n_1 values that give the correct coefficient of restitution, the shapes of the force against distance graphs for the impact closely resembled the experimental curves in Fig. 5. This single spring and damper model gives the same coefficients of restitution for different drop heights within a range of 0.1 to 1 m.

The modelling of the bending of the polystyrene cantilever is relatively straightforward because polystyrene is a low damping material. Therefore the initial slope of the experimental force deflection graph can be used ($k_2 = 45\,\mathrm{kN\,m^{-1}}$ under impact conditions). For an elastic cantilever of length $L = 30$ mm, width $w = 20$ mm and depth $d = 4.0$ mm, a Young's modulus $E = 4.0\,\mathrm{GN\,m^{-2}}$ gives a spring constant $k_2 = 47\,\mathrm{kN\,m^{-1}}$, confirming that this is a reasonable value for glassy polystyrene at high strain rates.

The damper constant n_2 is best estimated from the tan δ value of polystyrene at 20° C [15] which is approximately 0.01. This represents the energy loss per radian of sinusoidal deformation as a fraction of the maximum stored elastic energy. For a Voigt model of a spring and damper in parallel it can be shown [15] that the damping at an angular frequency ω is

$$\tan \delta = \omega\tau \qquad (17)$$

where the retardation time $\tau = n_2/k_2$. Therefore for the 40 mm long polystyrene beam which has a resonant vibration with period $T = 0.37$ msec, a value of $n_2 = 0.026\,\mathrm{Nsec\,m^{-1}}$ will produce a tan δ of 0.01.

Finally the effective mass M_2' of the specimen must be evaluated. The actual mass of a 40 mm long cantilever

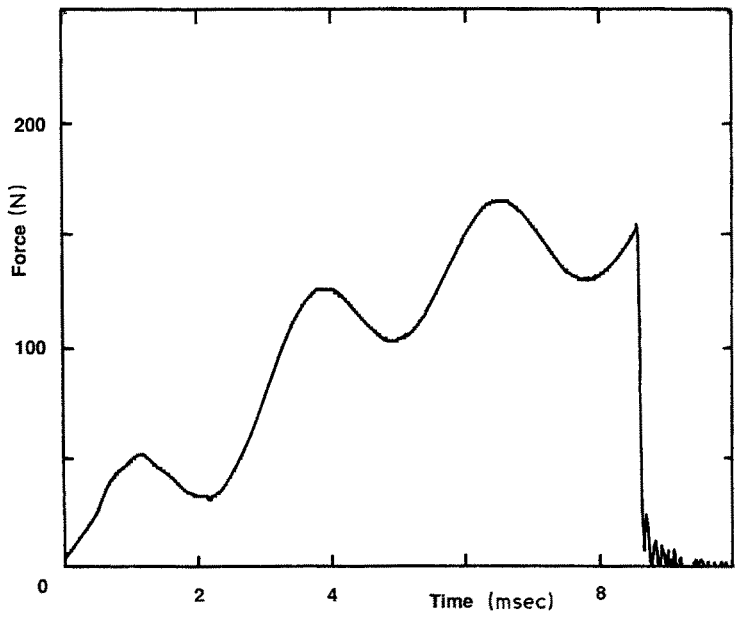

Figure 10 Striker force against time for a polystyrene Izod specimen of length 100 mm. Thin polyurethane layer on striker.

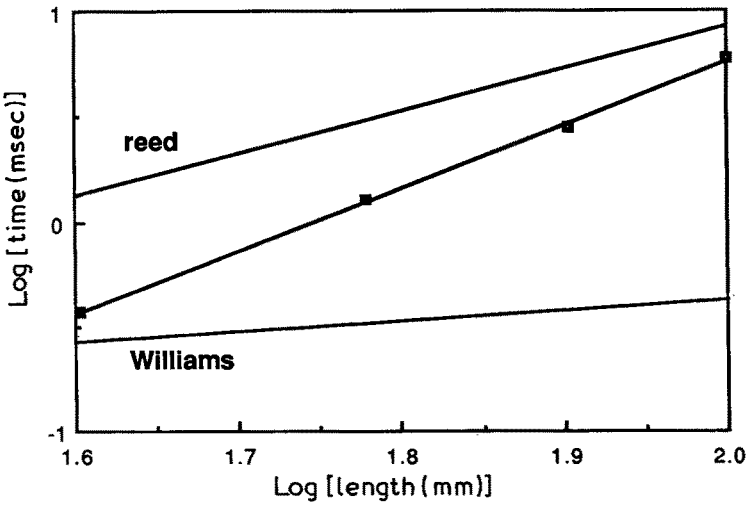

Figure 11 Variation of the oscillation period from traces like Fig. 10 with the cantilever length. The theoretical predictions of both the Williams' model for $k_1 = 750\,\mathrm{kN\,m^{-1}}$ and the vibrating-reed model are shown.

is 3.6 g. If the effective mass is defined in terms of equal momentum then it is 39% of the real cantilever mass. The final set of parameters for the modelling are set out in Table IV. The results of the computer simulation are shown in Fig. 12. For the steel striker simulation the initial impact peak of 85 N is equal to the experimental 90 N and the overall impression of a highly oscillatory trace is reasonable. However the size of the second and subsequent oscillations is too large, and the oscillations are damped out more rapidly than in the experiment. For the striker covered with the thin high modulus polyurethane the excessive damping of the oscillations is obvious; instead of five peaks being visible only the first and a minor second peak occur. For the striker covered with a thick rubber layer the predicted initial peak of 18 N agrees with a 15 N step increase in the experimental data but the shape after this initial peak differs.

Given that the computer simulations are a reasonable model of the experiment, some useful predictions can be made of quantities that were not measured experimentally. For example the force F_{23} transmitted to the Izod machine clamp can be predicted. Even under conditions where the force measured by the pendulum F_{12} is highly oscillatory the clamp force F_{23} increases nearly monotonically (Fig. 13). This suggests that another way of extracting a smooth force trace is to place the transducer at the clamp position. However there may be difficulties in avoiding errors caused by bending moments at the clamp, or changes in the clamping pressure.

4.5. Fracture surfaces and fracture parameters

The polystyrene bars develop a set of crazes on the tensile surface near the clamp. Eventually one of these crazes breaks. Fracture surface examination with a scanning electron microscope shows that one or other surfaces of the craze fail, i.e. a crack forms at the craze–bulk interface. Typically the craze extends the entire 20 mm width of the specimen and penetrates 2 to 3 mm through the thickness prior to fracture. There was no sign that the different contact conditions in the impact tests affected either the craze size or the detailed appearance of the fracture surfaces.

5. Discussion

One source of oscillations in instrumented impact tests was clearly shown to be flexural vibrations of the

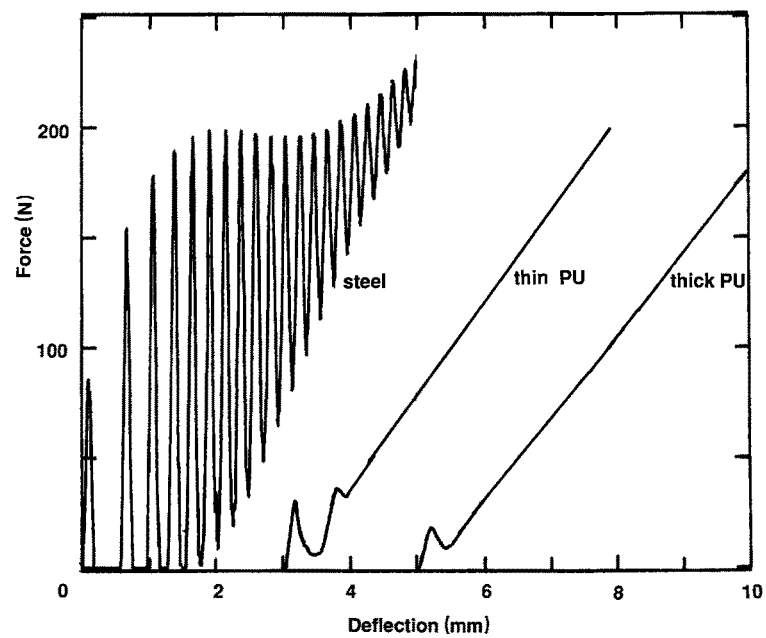

Figure 12 Computer model predictions of the striker force against deflection for impacts on 40 mm long polystyrene Izod beams, for the three contact conditions.

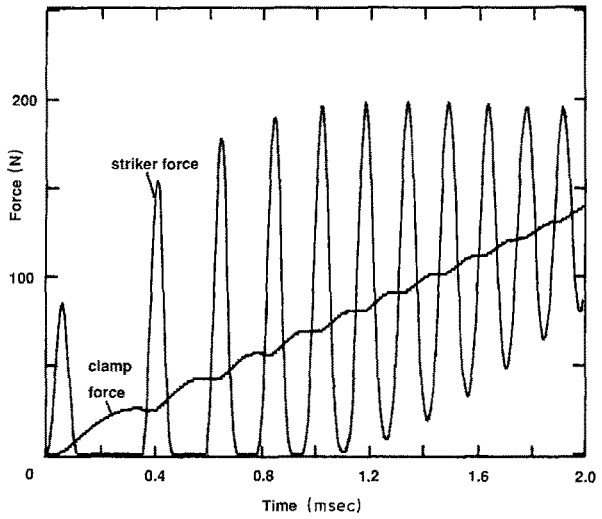

Figure 13 Predicted force against time variation for the steel striker condition of Fig. 12. Both the striker F_s and clamp F_m forces are shown.

sample. The initial cause of these oscillations is the impact between the steel striker and the specimen, and the magnitude of the initial peak was shown to be proportional to the impact velocity. While it is convenient in the laboratory to carry out impact tests at velocities in the range 1 to 3 m sec^{-1}, in real life the impact velocities can be much higher, so the corresponding force peaks can also be much greater. In general the contact stiffness between a steel striker and a plastic test bar will be high, so these oscillations will be an important feature of the test.

The Williams' theory for the force oscillations in impact tests uses three masses travelling along the same axis. The centre of gravity of the specimen lies on the line of travel of the striker; this implies a direct compressive impact with the specimen. It is not surprising therefore that the model fails to predict quantitatively the forces that occur when impacts occur on slender cantilever beams with a length to diameter ratio of 20 : 1. The model is qualitatively correct but it cannot predict flexural waves or flexural vibrations of the beam. Thus the measured period of oscillation only approaches the Williams' prediction for the beams with length to thickness ratios less than 8, and the predicted force peaks are twice the observed size for a slender beam. For the Izod tests, where the cantilever length to beam depth ratio is 8 : 1, the predicted peak heights are approximately correct. Izod and Charpy impact tests on plastics involve the bending of beams with differing length to thickness ratios, so it cannot be assumed that the Williams' model gives an quantitative prediction of the size or period of the initial oscillation. However the model is valuable in indicating the key variables involved, namely the impact velocity, the contact stiffness, and the effective mass of the specimen. The contact stiffness can be reduced by either reducing the contact area of the striker (there is a limit when the specimen starts to yield under the contact point) or by interposing a compliant layer such as a rubber. The effective mass of the specimen can be reduced by reducing the thickness of the specimen, but this may act against

TABLE IV Modelling of polystyrene Izod test

Quantity	Units	Contact condition		
		Steel	Thin rubber	Thick rubber
k_1	kN m^{-1}	2800	750	250
n_1	Ns m^{-1}	6	80	300
k_2	kN m^{-1}		45	
n_2	Ns m^{-1}		0.026	
M_2'	g		1.4	
F_L	N		100	

other features of the test design such as the required bending stiffness.

The vibrating cantilever beam or reed model assumes that the beam is slender, so that all of its deflection is due to longitudinal tensile strains rather than shear or compressive strains. It appears to predict the correct periods of oscillation for beams with length to thickness ratios exceeding 25. It is difficult however to take this approach further and develop a model of flexural waves in a viscoelastic beam. Possibly high speed photography could reveal the modes of vibration in the beams and whether the transmission and reflection of flexural waves is important.

We have shown that one effective method of removing oscillations from instrumental impact tests is to reduce the contact stiffness using a low modulus material of low coefficient of restitution. Just using a low modulus rubber between the striker and the specimen is not enough to remove the oscillations. It is a matter of judgement of how thick a rubber layer to use. To prevent errors in the beam deflection calculation of more than 10% the rubber should be as thin as possible. With the polystyrene beam geometry used 3 mm of rubber could be tolerated, but with a stiffer polymer beam the rubber would need to be thinner.

The successful modelling of the Izod impact tests allows some comments to be made on the use of the forces F_s exerted by the striker and F_m exerted by the machine support on the other end of the specimen. Some authors [4, 7] imply that one of these is the "force in the specimen", but this is a misleading concept. The reasons why F_s differs from F_m (Fig. 13) is that the specimen has a finite mass, and this mass can oscillate rapidly between the two much larger machine and striker masses. In order to calculate either the maximum stress for fracture in an unnotched specimen, or the stress intensity factor for crack growth in a cracked specimen, the bending moment at the fracture point must be known. For an Izod specimen which breaks near the clamp, the statics calculation of the bending moment involves the striker force F_s. For a Charpy specimen which breaks near the striker, the statics calculation involves the machine force F_m. However in an impact test lasting the order of 5 msec the accelerating specimen mass also produces a moment at the fracture position. Kalthoff [16] studied this problem in detail, carrying out Charpy tests on cracked epoxy thermoset bars. He showed that the force at the specimen support also oscillates, but is delayed in phase compared with the striker force

oscillations. This contrasts with the predictions of Williams' [4], or in Fig. 13 here, where the support force increases monotonically, in a series of steps. Kalthoff used the optical method of caustics to measure the dynamic stress intensity factor at the crack tip. This oscillates slightly and its phase lies between that of the striker and support forces; it is not possible to calculate it from some average of the striker and support forces. Therefore we suggest that an easier solution than using the method of caustics is to remove the cause of the striker force oscillations by changing the contact mechanics. This then reduces the specimen oscillations, and allows the calculation of the fracture stress, or stress intensity factor for a propagating crack, from the striker force.

For the polystyrene bars tested here it has been shown that reduction in impact oscillation effected by a rubber nose on the striker does not significantly alter the fracture force or the fracture energy input. On the other hand the fracture stress on a 5 msec time scale of $100 \pm 15\,\mathrm{MN\,m^{-2}}$ and the fracture strain of $3.1 \pm 0.6\%$ are more than double those measured in conventional tensile tests. Since fracture is preceded by extensive crazing this means that the craze stress must be of the order of $100\,\mathrm{MN\,m^{-2}}$ in an impact test, whereas estimates from the study of statically loaded crazes in 1 μm thick films lead to estimates as low as $20\,\mathrm{MN\,m^{-2}}$ [17]. It is clear that conventional UTS data is of little use in predicting the failure of a polystyrene product under impact conditions.

Acknowledgements

P.Z. is grateful to the British Council for support during a 6-month stay at Birmingham University.

References

1. CEAST booklet, "Advanced Fractoscope System MK 3", 1986, Torino, Italy.
2. ICI Australia Operations Ltd., booklet, "ICITACS Instrumented Impact Tester", 1986.
3. J. G. WILLIAMS and M. W. BIRCH, "Fracture 1977", ICF 4 Conference, Waterloo, Canada, Vol. 1, p. 501.
4. J. G. WILLIAMS and G. C. ADAMS *Int. J. Fracture* **33** (1987) 209.
5. J. S. MOOIJ, *Polymer Testing* (1981) 69.
6. P. J. HINE, R. A. DUCKETT and I. M. WARD, *J. Mater. Sci.* **21** (1986) 2049.
7. A. J. KINLOCH, G. A. GODOKIAN and M. B. JAMARANI, *ibid.* **22** (1987) 4111.
8. A. GALE and N. J. MILLS, *Plastics and Rubber Proc. Appl.* **5** (1985) 101.
9. A. GILCHRIST and N. J. MILLS, *J. Occupational Accidents* **9** (1987) 199.
10. K. W. HILLIER, *Proc. Phys. Soc.* **B64** (1951) 998.
11. I. M. WARD, "Mechanical Properties of Solid Polymers" (Wiley, London, 1971) p. 123.
12. G. C. ADAMS and T. K. WU, in "Fracture of Plastics", edited by W. Brostow and R. D. Corneliussen (Hanser, Munich, 1986) Ch. 8.
13. J. G. WILLIAMS, "Fracture Mechanics of Polymers" (Ellis Horwood, Chichester, 1984) p. 238.
14. *Idem, Int. J. Fracture* **33** (1987) 47.
15. N. J. MILLS, "Plastics" (Edward Arnold, London, 1986).
16. J. F. KALTHOFF, *Int. J. Fracture* **27** (1985) 277.
17. T. CHAN, A. M. DONALD and E. J. KRAMER, *J. Mater. Sci.* **16** (1981) 676.

Received 22 April
and accepted 5 September 1988